



SBGf Conference

18-20 NOV | Rio'25

Sustainable Geophysics at the Service of Society

In a world of energy diversification and social justice

Submission code: W78LV6BW7N

See this and other abstracts on our website: <https://home.sbgf.org.br/Pages/resumos.php>

Acoustic Image Logging as a Tool for Lithofacies and Silicification Analysis in the Pre-Salt Barra Velha Carbonates, Búzios Field

Isadora Dutra (Federal Fluminense University), Ana Carolina Carius (Fluminense Federal University), Ana Carla Pinheiro (Federal Fluminense University - GIECAR), Ricardo Jahnert (UFF), Francisco Abrantes Junior (Universidade Federal Fluminense), Wagner Lupinacci (GIECAR)

Acoustic Image Logging as a Tool for Lithofacies and Silicification Analysis in the Pre-Salt Barra Velha Carbonates, Búzios Field

Copyright 2025, SBGf - Sociedade Brasileira de Geofísica/Society of Exploration Geophysicist.

This paper was prepared for presentation during the 19th International Congress of the Brazilian Geophysical Society held in Rio de Janeiro, Brazil, 18-20 November 2025. Contents of this paper were reviewed by the Technical Committee of the 19th International Congress of the Brazilian Geophysical Society and do not necessarily represent any position of the SBGf, its officers or members. Electronic reproduction or storage of any part of this paper for commercial purposes without the written consent of the Brazilian Geophysical Society is prohibited.

Abstract

This study integrates acoustic image and geophysical well logs, and core descriptions from Well 9-BUZ-4-RJS in the Búzios Field, specifically for the Barra Velha Formation. We identified five acoustic facies and seven stratigraphic zones. The proposed facies show strong correlations with observed diagenetic alterations and the primary lithologies. Results indicate that vertical silica distribution in the well region is linked to late-stage fluid percolation, which is controlled by stratigraphic barriers and fault zones. This work advances understanding of silica-influenced carbonate reservoirs and provides a framework to identify these processes in wells with limited core data.

Introduction

Despite nearly two decades since its discovery, the characterization of Pre-Salt carbonate reservoirs continues to present challenges. While detailed core analysis could provide critical insights, its high operational cost often limits acquisition. In this context, borehole image logs (BHI) have emerged as an essential tool for reservoir evaluation and are now routinely acquired. Consequently, recent studies integrating BHI facies analysis with petrophysical and lithological data have advanced, aiming to establish correlations that reflect both the depositional fabric of carbonates and their overprinted diagenetic signatures (e.g., Muniz & Bosence, 2015; Lai et al., 2018; Basso et al., 2022). This study proposes a classification of five acoustic facies in the Barra Velha Formation, based on acoustic image logs, petrophysical data, and core samples from Well 9-BUZ-4-RJS. Located in the Búzios Field's Central High, the well was subdivided into seven stratigraphic zones, each distinctly affected by silicification with direct impacts on reservoir quality. This study hopes to assist in the application of image logs for Pre-Salt reservoir evaluation, especially where core data is limited.

Data and Methods

We classified acoustic image log facies in the well 9-BUZ-4-RJS based on textural aspects, static image amplitude, sedimentary structures, bedding patterns, and petrophysical properties. The study focuses on the Barra Velha Formation. Interpretation of acoustic facies involved the integration of core descriptions, conventional logs, Nuclear Magnetic Resonance (NMR), and Elemental Capture Spectroscopy (ECS). Macroscopic description was performed on approximately 175 m of core samples, equivalent to 95% of the studied section. When available, thin section analyses were used to complement these descriptions, with emphasis on rock texture and depositional fabric. The entire vertical extent of the Barra Velha Formation was logged by the image tool. This allowed depth calibration of the cores with reference to the acoustic image log. In general, we observed a good correlation between structures identified in the cores and those interpreted from image log.

Results

The core consists of 72% reworked carbonate facies, which are represented by grainstones (60%), rudstones (8%), and packstones (4%). The in-situ rocks consist of 12% mudstone lithofacies, while less than 13% of the interval includes shrubstones and spherulstones. The predominance of grainstone lithology over others influenced the dominant lithological

correspondence of facies 1, 2, 3, and 5. The acoustic facies identified, and their key features—including porosity and permeability properties, are presented in **Figure 1**.

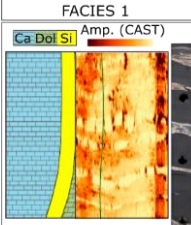
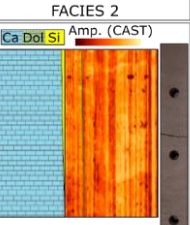
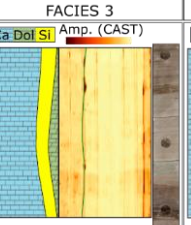
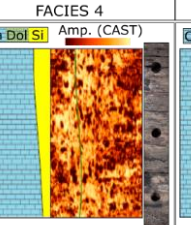
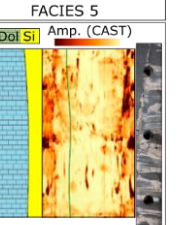
	FACIES 1	FACIES 2	FACIES 3	FACIES 4	FACIES 5
					
DESCRIPTION	Thick beds with moderate amplitude and rough texture interbedded with centimeter-scale, sinusoidal to semi-continuous high-amplitude layers, occasionally fractured. Abrupt contact between beds.	Particulate to arbustiform apparent porosity, with moderate to low amplitude. Texture is rough and homogeneous, with thick and poorly defined layers. Dissolution features and isolated silica nodules aligned with bedding are common.	High amplitude and homogeneous texture. Commonly contains thin layers and transparent to faintly visible structures. Frequently intersected by breakouts and fractures.	Chaotic and very rough texture with abrupt amplitude variations. High apparent porosity, marked by numerous dissolution features such as vugs and caverns. Occasionally, vugs are aligned with bedding.	Mottled texture with irregular high- and low-amplitude areas that obliterate the rock's original structure. Dissolution features are smaller and less numerous than in Facies 4.
NMR	Average effective porosity: 16% Median permeability: 180 mD	Average effective porosity: 17% Median permeability: 570 mD	Average effective porosity: 9% Median permeability: 3 mD	Average effective porosity: 15% Median permeability: 78 mD	Average effective porosity: 11% Median permeability: 3 mD
MINERAL PROP.	Calcite (μ -Md): 80-82% Dolomite (μ -Md): 7-4% Silica (μ -Md): 13-11%	Calcite (μ -Md): 87-90% Dolomite (μ -Md): 6-1% Silica (μ -Md): 7-6%	Calcite (μ -Md): 75-77% Dolomite (μ -Md): 10-4% Silica (μ -Md): 16-15%	Calcite (μ -Md): 84-87% Dolomite (μ -Md): 5-0,1% Silica (μ -Md): 11-10%	Calcite (μ -Md): 75-75% Dolomite (μ -Md): 3-0,1% Silica (μ -Md): 22-23%
CORRESPONDENCE	Dominated by Grainstone (71%), with secondary occurrence of Spherulite (10%). It contains a considerable percentage of the total rocks described as spherulite (36%), breccia (23%), and shrubstone (16%).	Dominated by grainstone, which accounts for the highest percentage of the lithology in this facies (39%), as well as for spherulite (47%) and breccia (45%). Shrubstone also makes a significant contribution (37% of the total lithology). Displays lithological diversity of reworked rocks, including rudstones, packstones, and mudstones.	Mudstone is concentrated in this facies (47% of the total lithology), although the dominant lithology within the facies is grainstone (56%).	Rudstone and shrubstone are the main components (43% and 32% of the facies, respectively). The highest proportion of both lithologies is also found within this facies.	Dominated by grainstone (75% of the facies) and secondarily by rudstone (11%) and breccia (10%). The second-highest occurrence of breccia is present in this facies.

Figure 1: Description of the main characteristics of the identified acoustic facies. The image logs represent 1 m of the borehole wall.

Facies 1 and 5 show spatial relationship and similarities regarding silicified intervals. Facies 1 is characterized by sinuous, fractured, silica-rich layers that in some regions are crosscut by faults, fractures, and more irregular distribution of silicified zones identified as facies 5. This pattern mainly affects initially porous rocks like grainstone and rudstone. In facies 5, pervasive silicification considerably reduced average permeability. Together, facies 1 and 5 represent over 50% of breccia occurrences.

Facies 2 exhibits the highest average calcite values and best permo-porosity characteristics. It is associated with reworked carbonates, a significant presence of shrubstone, and well-preserved original porosity. Silica occurs locally as cement, clasts, or isolated nodules.

Facies 3 is composed of 77% grainstone and rudstone, showing original porosity intensely cemented. This facies contains 47% of mudstone samples, distinguishable mainly by gamma ray peaks. Some thin sections reveal dolomite and microcrystalline silica replacing the former clay matrix. The high silica and dolomite content, associated with low permeability and high acoustic amplitude, reflect intense cementation of lithologies from different depositional environments.

Facies 4 is primarily diagnosed by dissolution features, randomly distributed vugs, giga- to megapores, or fenestral porosity aligned with bedding. Poorly sorted rudstones and shrubstone are the main associated lithologies, though it is poorly sampled in thin sections and core. In image logs, abrupt amplitude variations associated with slightly increased dolomite or silica proportions suggest active dissolution and cementation processes.

Seven stratigraphic zones were defined based on bedding direction, acoustic facies, and depositional characteristics (Figure 2).

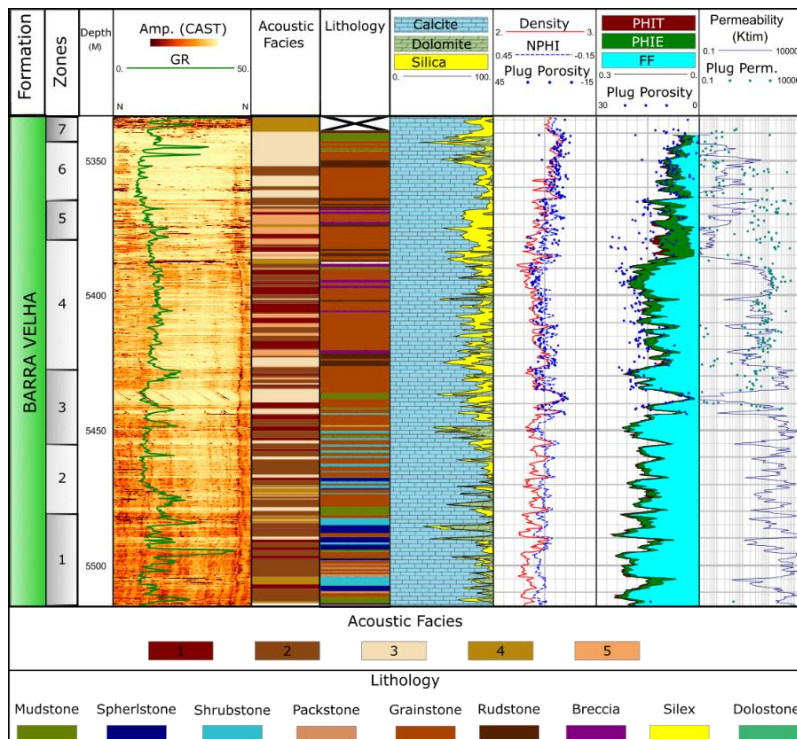


Figure 2: Zonation, facies classification, core description, and interpreted geophysical logs from this study for well 9-BUZ-4-RJS.

Discussions

The interpretation of the acoustic facies revealed a strong correlation between predominant diagenetic alterations and the permo-porosity distribution in the studied intervals. Silica distribution varies along the well and has significant implications for reservoir quality. The lower zones (1 to 3) are the least affected by silicification and correspond to the best reservoir intervals, with high permo-porosity associated with the dominance of acoustic Facies 2.

Silica occurrence is concentrated in Zone 4 and 5, characterized by breccias, fractures, and high silica content intervals linked to Facies 1 and 5. In Zone 4, silica exhibits a stratiform and sinuous pattern (Facies 1), following the bedding of reworked rocks. In Zone 5, pervasive silicification (Facies 5) suggests the action of silica-rich fluids channeled through fault and fracture systems during late diagenetic stages (Lima & De Ros, 2019; La Bruna et al., 2021). These two silica types correspond to type I (stratiform) and type II (pervasive), as described by Fernández-Ibáñez et al. (2022). The spatial relationship between them observed in this study aligns with the conceptual framework proposed by those authors. Two possible events may explain the observed pattern: (i) remobilization of silica I as a potential source for silica II, enhanced by fractures and faults; (ii) external input of silica II by hydrothermal fluids restricted to fault zones.

Although the thick silica layers associated with silica I and facies 1 are interpreted as being of syndepositional/eodiagenetic origin, resulting from changes in lake chemistry (Tosca & Wright, 2018; Fernández-Ibáñez et al., 2022), the nearby occurrence of faults raises the possibility of a hydrothermal origin. Conceptual models of stratigraphy-controlled hydrothermal flow have already been discussed for similar settings (Souza et al., 2021; Basso et al., 2023). Additionally, Zones 3 and 6, which bound the silica-rich zones, exhibit layers with abrupt permeability drops. These units may have acted as stratigraphic barriers, limiting the vertical extent of silicification.

Conclusions

The integrated analysis of acoustic image logs, core descriptions, and geophysical well logs allowed the identification of five acoustic facies and seven stratigraphic zones within the Barra Velha Formation in Well 9-BUZ-4-RJS. Pervasive silicification and hydrothermal fluid circulation were found to have a significant impact on reservoir quality. The vertical distribution of silica indicates hydrothermal fluid channelization through fractures and faults in Zone 5, while suggesting potential stratigraphic control by Zones 3 and 6 over the vertical extent of fluid percolation. These findings suggest a strong structural and stratigraphic control on the distribution of diagenetic alterations. The approach adopted in this study proved effective in capturing the vertical heterogeneity of the reservoir and in identifying key diagenetic processes affecting Pre-Salt carbonates, within the resolution limits of the available data. Furthermore, the proposed textural classification provides a useful framework for future paleoenvironmental and diagenetic interpretations of the Barra Velha Formation.

Acknowledgments

The authors thank Petrobras for financial support and the ANP for providing the data.

References

Basso, M., Chinelatto, G. F., Belila, A. M. P., Mendes, L. C., Souza, J. P. P., Stefanelli, D., Vidal, A. C., & Bueno, J. F. (2023). Characterization of silicification and dissolution zones by integrating borehole image logs and core samples: a case study of a well from the Brazilian pre-salt. *Petroleum Geoscience*, 29(3). <https://doi.org/10.1144/petgeo2022-044>

Basso, M., Souza, J. P. P., Honório, B. C. Z., Melani, L. H., Chinelatto, G. F., Belila, A. M. P., & Vidal, A. C. (2022). Acoustic image log facies and well log petrophysical evaluation of the Barra Velha Formation carbonate reservoir from the Santos Basin, offshore Brazil. *Carbonates and Evaporites*, 37(3). <https://doi.org/10.1007/s13146-022-00791-4>

Fernández-Ibáñez, F., Jones, G. D., Mimoun, J. G., Bowen, M. G., Simo, J. A., Marcon, V., & Esch, W. L. (2022). Excess permeability in the Brazil Pre-Salt: Nonmatrix types, concepts, diagnostic indicators, and reservoir implications. *AAPG Bulletin*, 106(4), 701–738.

La Bruna, V., Bezerra, F. H. R., Souza, V. H. P., Maia, R. P., Auler, A. S., Araujo, R. E. B., Cazarin, C. L., Rodrigues, M. A. F., Vieira, L. C., & Sousa, M. O. L. (2021). High-permeability zones in folded and faulted silicified carbonate rocks – Implications for karstified carbonate reservoirs. *Marine and Petroleum Geology*, 128. <https://doi.org/10.1016/j.marpetgeo.2021.105046>

Lai, J., Wang, G., Wang, S., Cao, J., Li, M., Pang, X., Han, C., Fan, X., Yang, L., He, Z., & Qin, Z. (2018). A review on the applications of image logs in structural analysis and sedimentary characterization. In *Marine and Petroleum Geology* (Vol. 95, pp. 139–166). Elsevier Ltd.

Lima, B. E. M., & De Ros, L. F. (2019). Deposition, diagenetic and hydrothermal processes in the Aptian Pre-Salt lacustrine carbonate reservoirs of the northern Campos Basin, offshore Brazil. *Sedimentary Geology*, 383, 55–81. <https://doi.org/10.1016/j.sedgeo.2019.01.006>

Muniz, M. C., & Bosence, D. W. J. (2015). Pre-salt microbialites from the Campos Basin (offshore Brazil): Image log facies, facies model and cyclicity in lacustrine carbonates. *Geological Society Special Publication*, 418(1), 221–242. <https://doi.org/10.1144/SP418.10>

Souza, V. H. P., Bezerra, F. H. R., Vieira, L. C., Cazarin, C. L., & Brod, J. A. (2021). Hydrothermal silicification confined to stratigraphic layers: Implications for carbonate reservoirs. *Marine and Petroleum Geology*, 124. <https://doi.org/10.1016/j.marpetgeo.2020.104818>

Tosca, N. J., & Wright, V. P. (2018). Diagenetic pathways linked to labile Mg-clays in lacustrine carbonate reservoirs: A model for the origin of secondary porosity in the Cretaceous pre-salt Barra Velha Formation, offshore Brazil. In *Geological Society Special Publication* (Vol. 435, Issue 1, pp. 33–46). Geological Society of London.